

Comparison of Four Technical Lignins as a Resource for Electrically Conductive Carbon Particles

Janea Köhnke,^{a,*} Notburga Gierlinger,^b Batirtze Prats Mateu,^b Christoph Unterweger,^c Pia Solt,^{a,c} Arnulf Kai Mahler,^d Elisabeth Schwaiger,^e Falk Liebner,^a and Wolfgang Gindl-Altmutter^a

Carbon microparticles were produced from different technical lignins, *i.e.*, kraft lignin, soda lignin, lignosulfonate, and organosolv lignin, at different carbonisation temperatures (800 °C, 1200 °C, 1600 °C, and 2000 °C). Before carbonisation, oxidative thermostabilization was performed. The combination of thermostabilization and carbonisation led to a high mass loss and shrinkage, but no major effect on the particle morphology was apparent. The carbon particles obtained from all four lignin variants developed disordered graphitic structures at high carbonisation temperatures, and good electrical conductivities in the carbon powders were observed for all lignin variants, with the exception of lignosulfonate. The polycaprolactone composite films filled with 30% lignin-derived carbon exhibited various conductivities, with the best results achieved using the kraft lignin-derived carbon.

Keywords: Lignin; Conductivity; Carbonisation; Carbon particles

Contact information: a: BOKU-University of Natural Resources and Life Science Vienna, Konrad Lorenz Strasse 24, A-3430 Tulln, Austria; b: BOKU-University of Natural Resources and Life Science Vienna, Muthgasse 11/II, A-1190 Wien, Austria; c: Wood K plus - Competence Center of Wood Composites and Wood Chemistry, Altenbergerstrasse 69, A-4040 Linz, Austria; d: Sappi Europe, Brucker Strasse 21, A-8101 Gratkorn, Austria; e: Mondi Paper Sales GmbH, Head of R&D Business Unit Packaging Paper, Frantschach 5, A-9413 St. Gertraud, Austria;

* Corresponding author: janea.koehnke@boku.ac.at

INTRODUCTION

Lignin, a major constituent in wood cell walls, is the second most abundant natural polymer after cellulose (Boerjan *et al.* 2003). When wood is digested in the pulp and paper industry with the aim of utilising cellulose and eventually hemicellulose, huge amounts of lignin become available as a secondary product from the pulping process. This results in an annual global lignin production of approximately 50 million tons (Gosselink *et al.* 2004). Because large-scale, high-value uses of lignin products are not available, lignin is mostly used for the production of heat and energy (Kai *et al.* 2016). With increasing prices for fossil oil and a growing trend towards renewable and sustainable resources, lignin becomes increasingly attractive as a potential low-cost source for value-added products. Consequently, there is an ongoing and steadily intensifying discussion about alternative usages of lignin, such as polymer production, biorefinery development, biofuels, and chemicals (Doherty *et al.* 2011; Chatterjee *et al.* 2014; Duval and Lawoko 2014; Laurichesse and Avérous 2014; Thakur *et al.* 2014; Xu *et al.* 2014; Bruijninx *et al.* 2015; Kai *et al.* 2016).

Currently there are four major technical lignins produced from pulping, which are kraft lignin (85% of the lignin produced worldwide (Tejado *et al.* 2007)), soda lignin (9%

(Sixta 2006)), lignosulfonate (6% (Mansouri and Salvadó 2006)), and organosolv lignin (not yet commercially available on a large scale). The structure, reactivity, molecular weight, and chemical composition of the resulting lignins are diverse. Kraft lignin originates from the sulphate cooking process, which involves sodium hydroxide and sodium sulphide as the main reagents (Chakar and Ragauskas 2004). The cooking liquor (black liquor) from this process contains fragments of lignin with different molecular weights (Betancur *et al.* 2009). It has high ash, hydroxyl, and carboxyl contents, as well as abundant condensed structures (Vainio *et al.* 2004). Soda lignin derives from the soda cooking process, which is free of sulphur (García *et al.* 2009). The soda cooking process is predominantly used for non-wood plants (grasses, bamboo, *etc.*) and only rarely applied to hardwood species (González-García *et al.* 2010). Hence, soda lignin is often characterised by high silicate and nitrogen contents (Rodríguez *et al.* 2010). Lignosulphonates arise from sulphite cooking processes. Acidic cooking liquor contains HSO_3^- and SO_3^{2-} with variable counter ions (Areskogh *et al.* 2010). In contrast with other technical lignins, lignosulphonates are water soluble because of sulphonation and degradation during the cooking process (Shulga *et al.* 2001). They show a high diversity in functional groups, some of which are charged. Compared with other technical lignins, lignosulphonates show a high molecular weight, high ash content, and low amounts of carbohydrates (Yang *et al.* 2007). Organosolv lignin is produced in a pulping process in which the cooking liquor contains water and organic solvents, *e.g.*, ethanol (Pan *et al.* 2005). Dissolved lignin characteristically has a low molecular weight (Çetin and Özmen 2002). Organosolv lignin has a high purity and is sulphur-free (Wang *et al.* 2009).

Lignin-derived carbon is an intensely researched route for generating additional value from technical lignins. In this context, potential applications include the substitution of fossil-based carbon black (Snowdon *et al.* 2014), lignin-based carbon fibres (Kadla *et al.* 2002; Ruiz-Rosas *et al.* 2010; Foston *et al.* 2013), carbon nanoparticles (Gonugunta *et al.* 2012), and activated carbon (Hayashi *et al.* 2000; Suhas *et al.* 2007). Recently it was determined that lignin-derived carbon particles may act as functional fillers in conductive polymers, similar to carbon black (Gindl-Altmutter *et al.* 2015; Ago *et al.* 2016; Köhnke *et al.* 2016; Köhnke *et al.* 2018). Carbon black is commercially produced by the thermal breakdown of hydrocarbons. Different processes lead to five different carbon blacks that are mass-produced (Bourrat 1993), and their particles vary considerably in terms of their shape, size, surface, conductivity, and porosity (Huang 2002). Different properties are important depending on the application, such as inks, polymer fillers (as reinforcing filler, conductive filler, stabilizer, antioxidant, pigment, and colorant), coatings, and electronic components (Balberg 2002).

In the present study, the suitability of four technical lignins as precursors for carbon microparticles were compared. In particular, the suitability of lignin-derived carbon as a functional, electrically conductive filler for polymers was evaluated. Here, lignin-based fillers could serve as a bio-based alternative to currently used conductive polymers such as polypyrrole (Das and Prusty 2012) and conductive polymer fillers such as carbon black (Jin *et al.* 2013) or carbon nanotubes (Castellino *et al.* 2016).

EXPERIMENTAL

Production of the Carbon Microparticles

Kraft lignin (Indulin AT) was purchased from MeadWestvaco (Richmond, USA). The lignin originated from a kraft cooking process of southern pine and was purified with acidic hydrolysis, where sodium and hemicelluloses were removed. Soda lignin (Protobind 2400), produced from wheat straw, was obtained from GreenValue (Alpnach Dorf, Switzerland). Softwood lignosulfonate (sodium lignosulfonate) was bought from Borregaard (Sarpsborg, Norway). The lignosulphonate was ultra-filtered, desulphonated, and oxidised. Organosolv lignin was provided by Fraunhofer (Leuna, Germany). Polycaprolactone (PCL) and toluene were purchased from Carl Roth GmbH & Co. KG (Karlsruhe, Germany). Treatment of the lignins began with a thermostabilization step that involved heating using a drying oven at an ambient atmosphere and a heating rate of 0.01 °C/min from 20 °C to 250 °C. Carbonisation was performed with four different target temperatures of 800 °C, 1200 °C, 1600 °C, and 2000 °C in a GERO HTK8 oven (Carbolite Gero, Sheffield, UK) with a volume of 6 L and an argon gas flow rate of 150 L/h. The heating rate was 1 °C/min up to 500 °C and was followed by a 1-h holding step. After that, the heating rate was increased to 5 °C/min, with a 1-h holding step at 900 °C and another 1-h holding step at the final temperature.

Characterisation of the Carbonised Lignin Particles

Scanning electron microscopy (SEM) was performed on a Quanta™ 250 field-emission environmental scanning electron microscope (FEI Europe B.V., Eindhoven, Netherlands) with a Schottky field emission gun at 10 kV and a high vacuum of 1×10^{-6} mbar. The samples were prepared on a copper conductive double-coated tab and were sputter-coated with a thin film of gold.

Elemental analysis was done on an elemental analyser (EA 1108 CHNS-O, Carlo Erba Instruments, Waltham, USA) at temperatures between 1020 °C and 1400 °C in tin capsules. Gas chromatography was used for separation with highest purity helium gas as a carrier. Quantification and detection were done with a thermal conductivity detector (6890GC with TCD, Agilent, Vienna, Austria).

Thermogravimetric analysis (TGA) and differential scanning calorimetry (DSC) were performed simultaneously on a Netzsch DSC 200 F3 Maia (Netzsch Group, Selb, Germany). Open aluminium crucibles were filled with carbon powder and heated at a rate of 5 °C/min under a nitrogen atmosphere.

The Raman spectra were measured on a Raman microscope (alpha300RA, WITec GmbH, Ulm, Germany) using a green laser ($\lambda = 532$ nm), a spectrometer with a 600-g/mm grating (UHTS 300, WITec GmbH, Ulm, Germany), and a charge coupled device camera (DU401ABV, Andor Technology, Belfast, UK). A laser power of 5 mW was used. With an integration time of 0.05 s, single spectra were collected every 250 nm over a region of $20 \mu\text{m} \times 20 \mu\text{m}$ (6400 spectra/region) using a 100x oil immersion objective (numerical aperture = 1.4). Finally, the average spectra of all four samples were calculated (19200 spectra/sample).

The electrical conductivity of the carbon powders was measured according to Sánchez-González *et al.* (2005). A plastic cylinder with an inner diameter of 6.22 mm was fixed onto a stationary metal piston. The cavity of the plastic cylinder was filled with 50 mg to 100 mg of carbon powder, up to a height of approximately 12 mm. The total height was measured and a second movable metal piston with the diameter the size of the cylinder

hole was inserted into the cylinder. Upon closure of the cylinder, various loads were applied to the upper piston to reach pressures of 65 kPa, 161 kPa, 226 kPa, 645 kPa, and 807 kPa. The conductivity and height of the powder were measured repeatedly after each increase in pressure. The conduction was ohmic; therefore, the electrical conductivity (σ ; $\Omega^{-1}\text{mm}^{-1}$) of the samples was calculated with Eq. 1 (Sánchez-González *et al.* 2005),

$$\sigma = l / (R \times A) \quad (1)$$

where l is the distance between the pistons (cm), R is the electrical resistance (Ω), and A is the area of the piston surface (m^2).

Polycaprolactone-carbon Composite Films

The PCL was dissolved in toluene at a concentration of 100 g/L under constant stirring at room temperature. The carbon particles were blended into the PCL and toluene mixture at a ratio of 30% carbon (mass) to 70% PCL (mass). The compound was decanted into a crystallising dish, and the toluene evaporated overnight. After 2 h in a vacuum drying chamber, the compound was folded and hot-pressed twice at 90 °C to achieve a more homogeneous and even distribution of carbon particles.

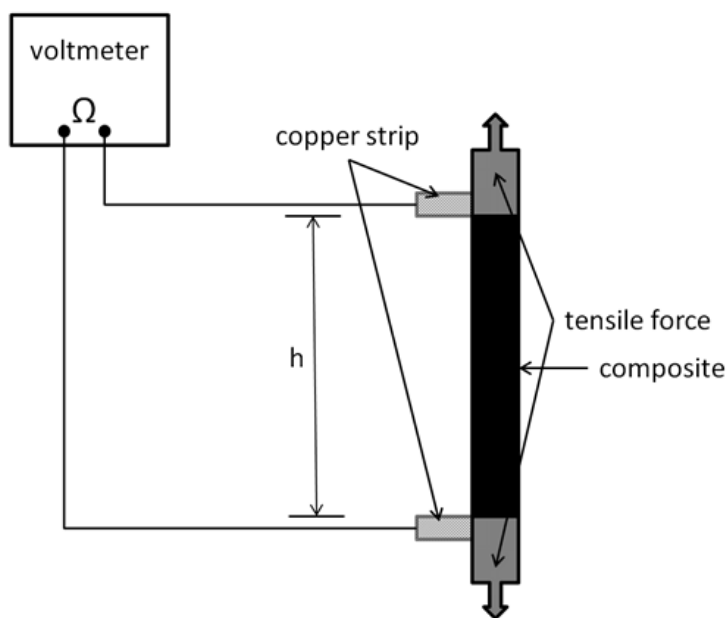


Fig. 1. Experimental device for the resistivity measurements of the composites during tensile loading

Thereafter, the composite was cut into strips 80 mm in length and 8 mm in width and inserted into a Zwick Roell 20-kN universal testing machine (Ulm, Germany) with a 2.5-kN load cell for tensile testing, as is seen in Fig. 1. For the resistivity measurements, two copper strips were added between the composite and grip at a distance (h) of 35 mm. The resistivity was measured during tensile loading.

RESULTS AND DISCUSSION

Gravimetric Yield and Structural Changes during Carbonisation

Overall, considerable mass losses occurred during all of the thermal treatment stages in the present study. Thermostabilization in an ambient atmosphere was performed to avoid fusing the lignin particles because of the inherent thermoplasticity of lignin during carbonisation (Braun *et al.* 2005; Norberg *et al.* 2013). The mass loss resulting from this treatment varied considerably for the four types of lignin (Fig. 2). With a 35% mass loss, lignosulfonate was most stable, whereas organosolv lignin showed the highest mass loss at 61%. During thermostabilization, a number of processes contributed to the mass loss. First, the initial mass loss was caused by the removal of moisture. Thereafter, the oxidation of lignin caused further mass loss that was associated with the loss of phenolic, alcoholic, methyl, carbonyl, and methoxyl groups (Braun *et al.* 2005; Norberg *et al.* 2013). While these phenomena primarily led to a loss of oxygen, hydrogen, and carbon, the inorganic compounds were not affected. This might have contributed to the fact that the organosolv lignin, which was virtually free of inorganics, showed the highest mass loss during thermostabilization.

The carbonisation treatment under an argon atmosphere, which followed thermostabilization, caused remarkable additional mass loss. For all of the lignins, severe mass loss was observed after the first two carbonisation steps with the target temperatures of 800 °C and 1200 °C, whereas only minor mass changes occurred at the higher temperatures (Fig. 2). In principal, mass loss during carbonisation is caused by the breaking of bonds, first the weaker bonds (*e.g.*, C-OH or hydrogen bonds) and then the stronger ones (*e.g.*, β -O-4 linkages), which directs the depolymerisation of lignin (Liu *et al.* 2015). Random repolymerisation of the remaining carbon structures occurs following depolymerisation and leads to graphitic and graphite-like structures (Song *et al.* 2017; Yi *et al.* 2017).

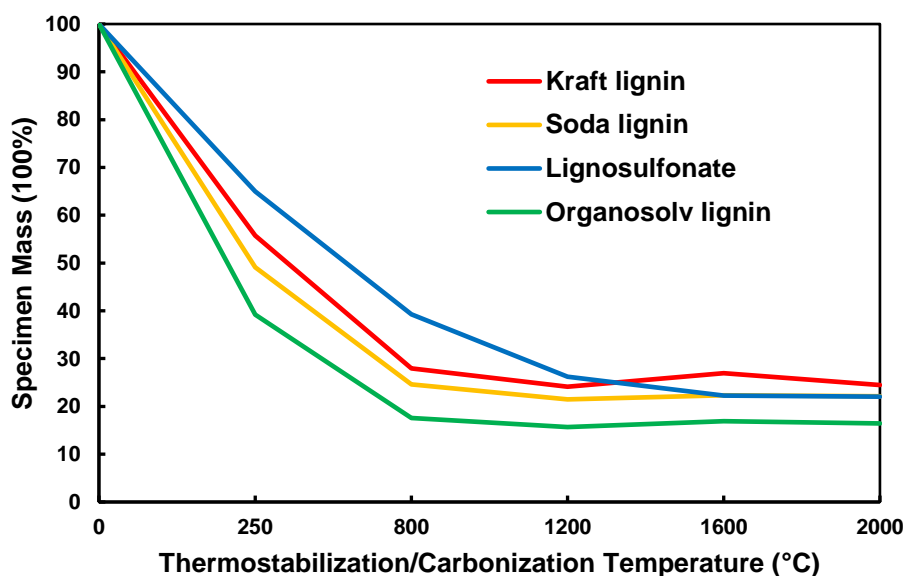


Fig. 2. Mass loss for all of the lignin samples during the thermal treatment of thermostabilization (250°C) and carbonization (800 °C and higher)

Table 1 shows an overview of the changes in the elemental composition of the four lignin variants used and compared the untreated lignin and specimens carbonised at 2000 °C. Regardless of the initial elemental composition, the carbon content of all of the lignin-derived carbons was above 99%, which indicated that inorganics were also largely volatilised at high carbonisation temperatures, which contributed to the overall mass loss. Trace amounts of inorganics, that were not detected in the untreated lignins, appeared after carbonisation, which was probably caused by impurities present in the carbonisation oven or graphite containers used during the carbonisation experiments.

Table 1. Elemental Analysis of the Untreated Lignins and Lignins Carbonised at 2000 °C

Material		Element (% w/w)							
		C	H	N	S	K	Na	Ca	Mg
Kraft lignin	untreated	62.8	5.8	0.9	0.1	-	-	-	-
	2000 °C	99.9	< 0.05	< 0.05	< 0.02	0.03	0.03	0.05	< 0.02
Soda lignin	untreated	61.9	5.9	0.9	< 0.02	-	-	-	-
	2000 °C	99.2	< 0.05	< 0.05	0.23	0.03	0.03	0.03	< 0.02
Lignosulfonate	untreated	47.9	3.7	0.2	2.0	-	-	-	-
	2000 °C	99.6	< 0.05	< 0.05	0.04	< 0.02	< 0.02	0.06	< 0.02
Organosolv lignin	untreated	61.1	5.9	0.3	< 0.02	-	-	-	-
	2000 °C	99.6	< 0.05	< 0.05	< 0.02	0.05	< 0.02	0.03	< 0.02

Simultaneous TGA and DSC analysis provided more information on the dynamics of the thermal decomposition over a limited temperature range of 600 °C (Fig. 3). Notably, the mass loss measured at 250 °C during TGA was less than the mass loss observed during thermostabilization. This was easily explained by the fact that TGA was done in a nitrogen atmosphere to prevent oxidation, whereas thermostabilization was performed with the intention of slow oxidation and thus inherently caused more mass loss than the TGA.

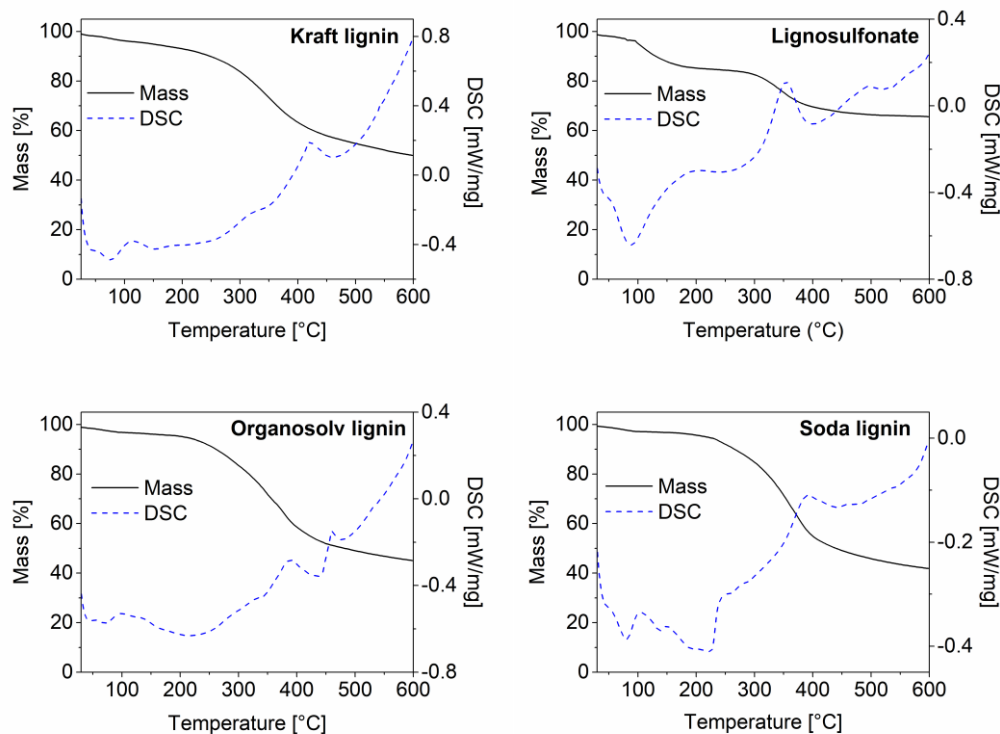


Fig. 3. TGA and DSC curves of all four untreated lignins: (a) kraft lignin; (b) lignosulfonate; (c) soda lignin; and (d) organosolv lignin

After a small initial mass loss because of moisture evaporation, a major mass loss began in the TGA between 200 °C and 300 °C and continued until 400 °C (Fig. 3). While this general trend applied to three of the lignins, lignosulfonate somewhat differed in that a first major mass loss was already seen at lower temperatures of 100 °C and 170 °C. The DSC analysis that was done simultaneously revealed the exothermal behaviour of the concurrent major mass loss in the temperature region of 300 °C to 400 °C. This exothermal peak was the most intense for lignosulphonate and was probably caused by the release of SO₂ during thermal degradation, which released the energy recorded during DSC (Köhnke *et al.* 2018). This high decomposition intensity of the lignosulfonate correlated well with the observation that out of all of the lignins, lignosulfonate showed the highest mass loss between the end of the thermostabilization phase and the final carbonisation step at 2000 °C (Fig. 2).

The Raman spectroscopy provided information about the degree of graphitic order in the carbon structures (Fig. 4). The Raman data showed the typical spectra of a graphitic lattice, which confirmed that carbonaceous structures were produced in the heating process (Dresselhaus *et al.* 2010). The G-band at approximately 1580 cm⁻¹, which corresponded to the single graphite crystal or ideal graphitic lattice, and the D-band at approximately 1350 cm⁻¹, which indicated the presence of polycrystalline graphite and therefore a disordered graphitic lattice, were the most important signals (Tuinstra and Koenig 1970; Sadezky *et al.* 2005). All of the lignin-derived carbon samples produced in the present study were characterised by a higher D-peak compared with the G-peak. This indicated that a noticeable degree of disorder was present in the graphitic structures. An evaluation of the ratio of the peak intensities that is shown in Fig. 4 indicated only minor differences between the four lignin-derived carbons. Among the carbons studied, lignosulfonate showed the

lowest G-band intensity compared with the D-band intensity, which was in good agreement with the specific thermal decomposition behaviour of this technical lignin variant (Köhnke *et al.* 2018). In contrast, for the carbon derived from spray-dried kraft black liquors, a clear dominance of the G-band over the D-band was observed by Köhnke *et al.* (2018), which indicated a high degree of graphitic order.

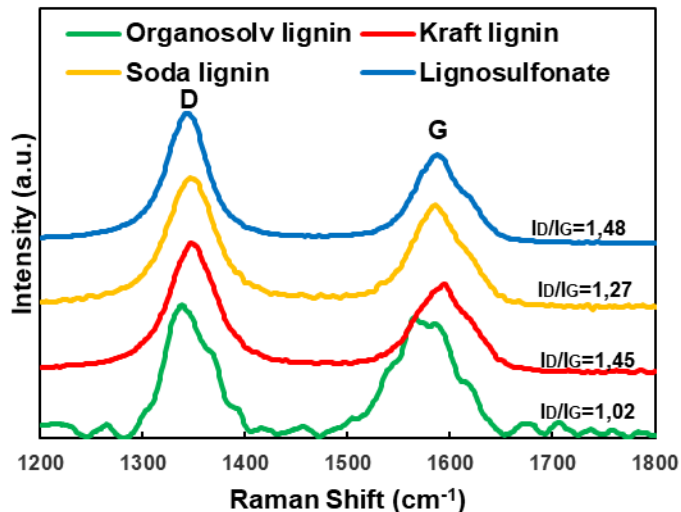


Fig. 4. Raman spectra of the lignin-derived carbon particles carbonised at 2000 °C

Morphological Characterisation by SEM

The different lignins received showed high variable particle sizes and particle morphologies, as is shown in Figs. 5 to 8.

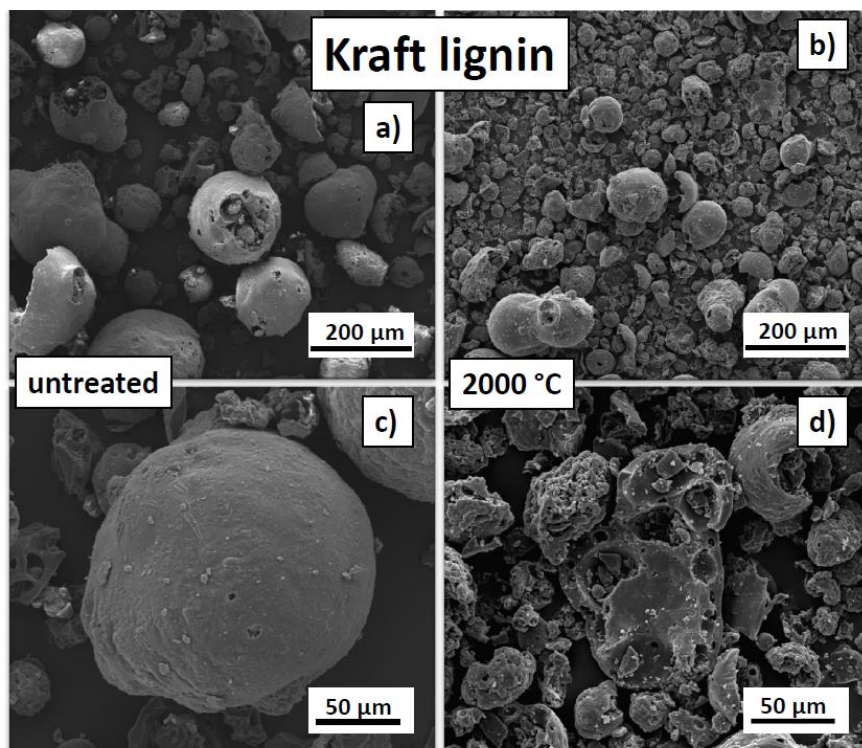


Fig. 5. SEM images of the untreated (a and c) and carbonised (2000 °C) kraft lignin (b and d)

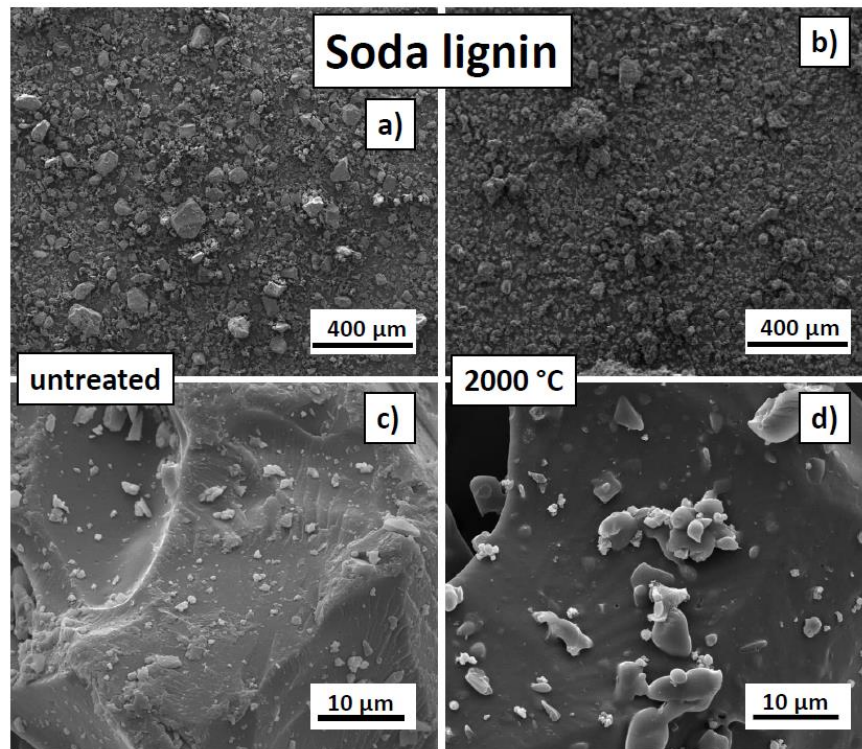


Fig. 6. SEM images of the untreated (a and c) and carbonised (2000 °C) soda lignin (b and d)

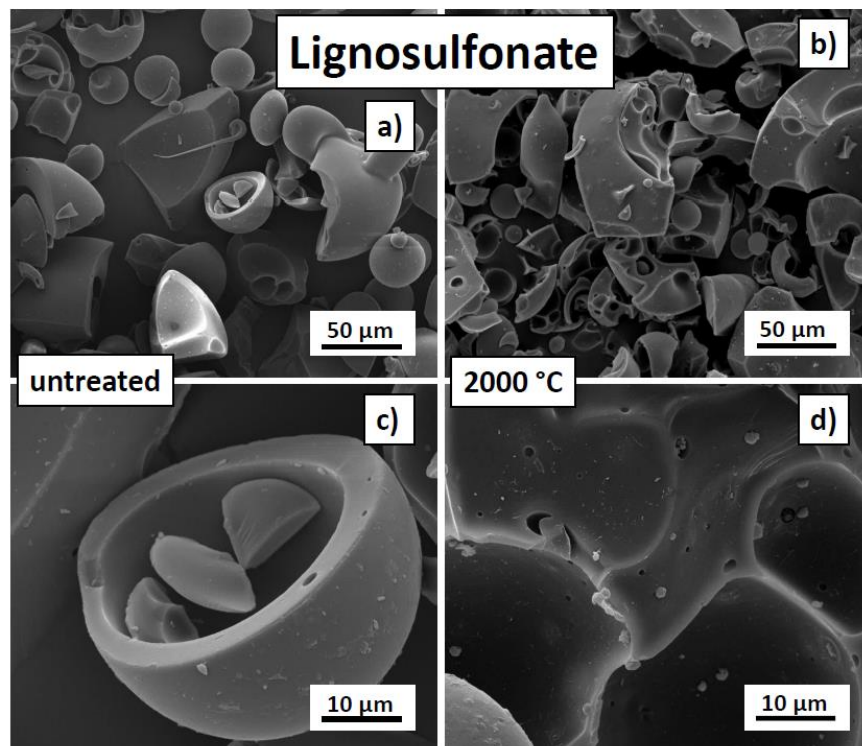


Fig. 7. SEM images of the untreated (a and c) and carbonised (2000 °C) lignosulfonate (b and d)

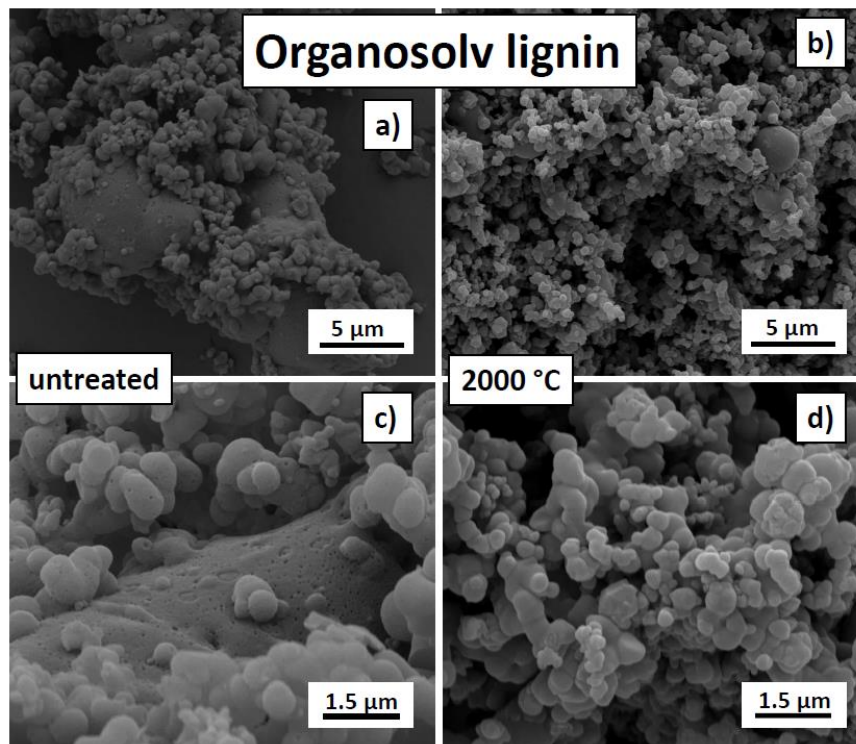


Fig. 8. SEM images of untreated (a and c) and carbonised (2000 °C) organosolv lignin (b and d)

The kraft lignin particles were spherical in shape and had internal cavities (Fig. 5). The particles had a broad particle size distribution with an average size of 59.0 µm, which was the largest diameter of all four lignin variants studied. After carbonisation, the particles shrank to an average diameter of 25.5 µm, which corresponded to a 56.8% shrinkage, which was the highest shrinkage of all of the lignins. Other than the shrinkage, small spots with high electron density contrast crumbs that adhered to the particle surfaces was the only apparent difference after carbonisation. These spots are most probably agglomerations of inorganic residues originating from wood constituents or process chemicals used during pulping (Köhnke *et al.* 2016).

Compared with all of the other lignins, the soda lignin was characterised by an irregular particle morphology, which indicated that it was probably milled (Fig. 6). Furthermore, the particles did not reveal any porosity detectable at the resolution used during SEM. The untreated soda lignin particles had a wide-ranging particle size distribution, with an average size of 14.2 µm, as is displayed in Fig. 6. After carbonisation, the particles shrank to 12.8 µm, which was an average shrinkage of 10.3%. This was the lowest shrinkage of all of the lignins and might have correlated with the absence of noticeable micropores in the particles. Other than shrinkage, no morphological changes because of carbonisation were observed.

The lignosulfonate observed by SEM (Fig. 7) appeared to be fragments of initially spherical, hollow particles. The surface of the fragments had a smooth appearance and porosity was present in small amounts. The size and wall thickness of the fragments showed a high variability. The untreated lignosulfonate particles had a particle size distribution with an average equivalent diameter of 46.2 µm. After carbonisation, the particles shrank to 30.2 µm, which was an average shrinkage of 34.7%. In addition to

considerable shrinkage, a clearly visible increase in the porosity occurred during carbonisation (Fig. 7).

The organosolv lignin particle morphology was different compared with the morphologies of the other three lignins, in that it consisted of particles of two different size classes (Fig. 8). Agglomerates with a characteristic size of 30 μm to 35 μm were apparent. Upon closer inspection, these agglomerates consisted of small lignin spheres with smooth surfaces and occasionally hollow structures. These small spheres had an average particle size of 0.5 μm and shrank down to 0.3 μm after carbonisation, which was a shrinkage of 39.7%. Those were the smallest particles found in this study. After carbonisation, changes in the morphology were absent.

Electrical Conductivity of the Carbon Powders and Carbon-polycaprolactone Composite Films

The electrical conductivity was determined for all of the samples, with the exception of the untreated and thermostabilised lignin. Because the conductivity of carbon powders varies with their density (Sánchez-González *et al.* 2005), measurements were taken at different pressures applied to the powders. The change in the conductivity as a result of increasing pressure was determined for the carbons derived from the four technical lignins using the carbons treated at 2000 °C (Fig. 9). All of the characterised specimens showed a roughly linear increase in the conductivity with an increasing pressure. Notably, the densities of the carbon powders were different, with the soda lignin-derived particles showing the highest density and organosolv-derived powder showing the lowest density. The high density of the soda-derived powder correlated with the morphology and pore-free characteristic of the particles (Fig. 6).

The values measured at a fixed pressure of 807 kPa were used for comparing the different lignin variants at all of the carbonisation target temperatures (Fig. 10). The lignosulfonate-derived carbon powder stood out with an electrical conductivity 10 times lower than that of the other carbon powders (Fig. 10). While all of the other carbon types showed a measurable, albeit moderate, electric conductivity at the first carbonisation target temperature of 800 °C, lignosulfonate carbon only appeared to be electrically conductive when prepared at 1600 °C and higher. Even then, a comparably lower level of conductivity was measured. This result was in good agreement with the carbonisation experiments done with spray-dried lignosulfonate liquor, where it was shown that a low degree of graphitic structure in this type of lignin-derived carbon correlated with the comparably low electrical conductivity (Köhnke *et al.* 2018). The hypothesis was put forward that due to the specific chemistry of lignosulfonate, substantial amounts of SO_2 are released during carbonization, which severely degrade the lignin structure, preventing formation of polycyclic moieties required for the build-up of graphitic structures.

The three other lignin-derived carbon powders showed comparable electrical conductivity values. With a characteristic conductivity in the order of 500 $\Omega^{-1}\text{mm}^{-1}$, the lignin-derived carbons produced in the present study showed clearly inferior performances to those of industrially produced carbon black, with conductivities in the order of 40 x 10³ $\Omega^{-1}\text{mm}^{-1}$ and up to 250 x 10³ $\Omega^{-1}\text{mm}^{-1}$ measured with a comparable set-up (Sánchez-González *et al.* 2005).

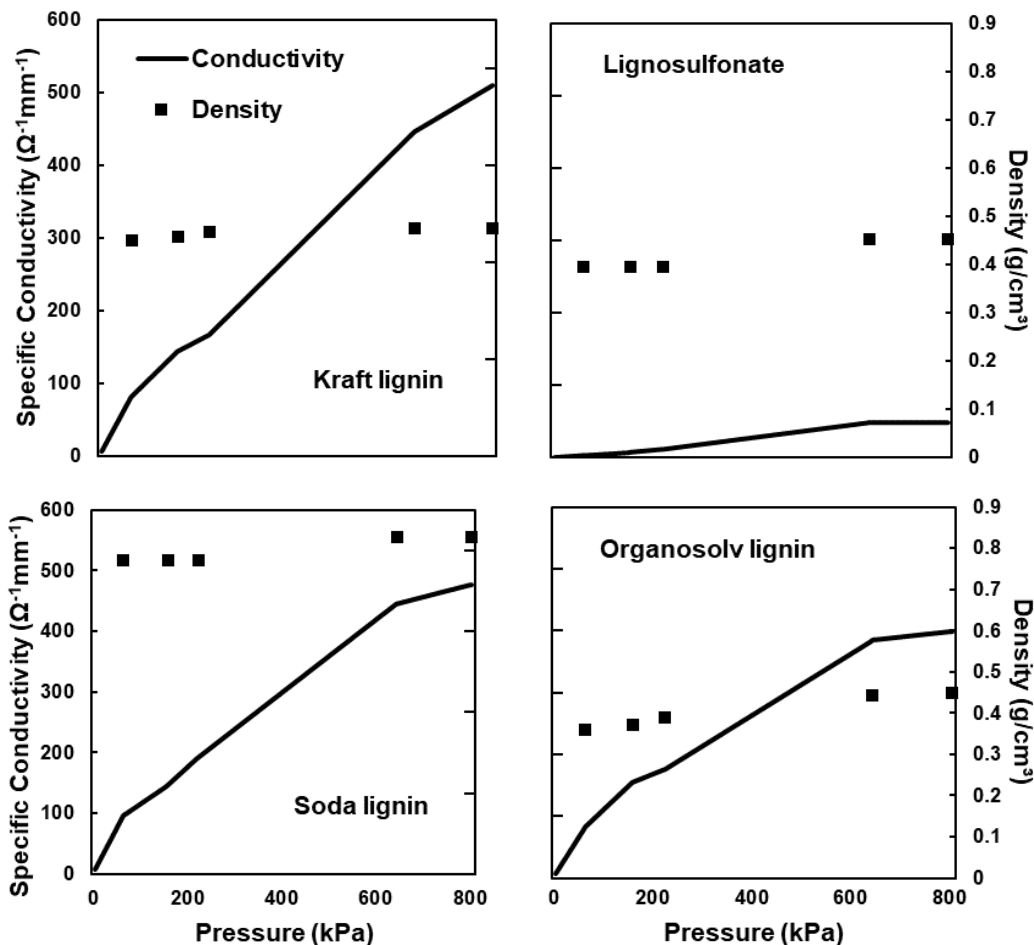


Fig. 9. Electrical conductivity of the four different lignins carbonised at 2000 °C with different pressures, as well as the parallel evolution of density: (a) kraft lignin; (b) lignosulfonate; (c) soda lignin; and (d) organosolv lignin

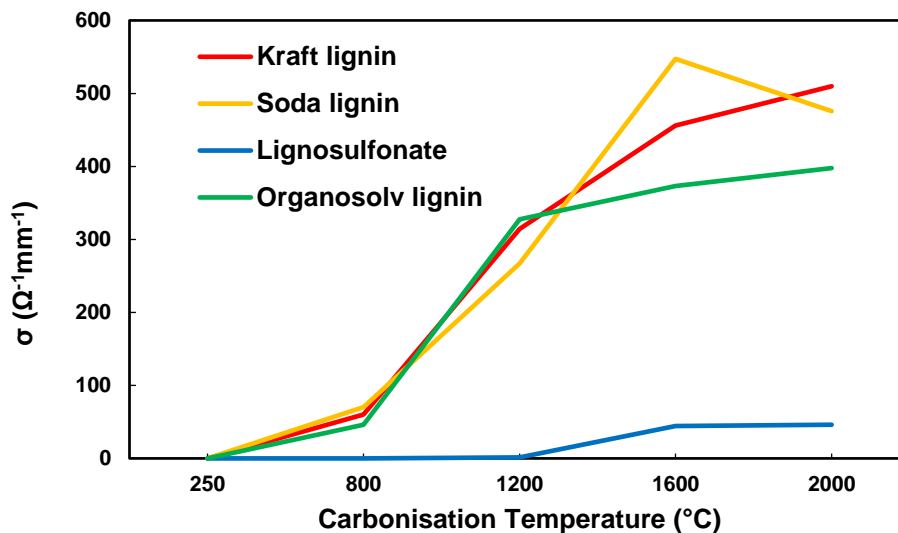
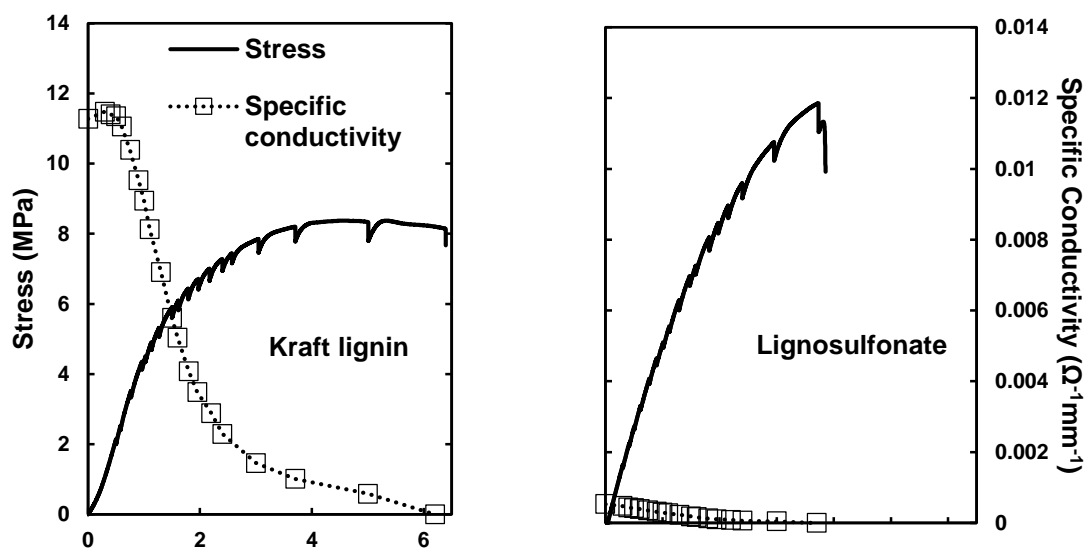


Fig. 10. Electrical conductivity of the four different lignins with different carbonisation temperatures and a pressure of 807 kPa

Having established that carbon powders derived from lignin showed electrical conductivity in principle, their suitability as functional fillers in a polymeric matrix was evaluated using PCL composites. Because of the comparably poor electrical conductivity, remarkable amounts (greater than 20% mass) of carbon needed to be added to the polymer to achieve electrical conductivity (Li *et al.* 2000; Gindl-Altmutter *et al.* 2015; Köhnke *et al.* 2016). Therefore, the PCL films were produced with a 30% carbon content for all of the lignin powders carbonised at 2000 °C, which were the carbon variants that showed the best conductivity (Fig. 10). Polycaprolactone was chosen as the matrix polymer because of its easy handling, biodegradability, and wide range of applications, such as in the biomedical and packaging industries (Woodruff and Hutmacher 2010). Polycaprolactone is a comparably soft and highly extensible polymer, which was confirmed by means of tensile testing (Table 2). As was expected based on the effect of particulate fillers in polymers in general (Fu *et al.* 2008), the addition of the particulate carbon filler resulted in a reduced strength and elongation at break, as well as an increase in the initial modulus of elasticity in most cases (Table 2).

Table 2. Properties of a Pure Polycaprolactone (PCL) Film Compared to the Properties of PCL Filled with 30% Carbon Content

	Modulus of Elasticity (MPa)	Tensile Strength (MPa)	Strain at Failure (%)
Kraft lignin	347 ± 32	6.59 ± 0.12	9.83 ± 2.27
Soda lignin	382 ± 19	9.09 ± 0.08	2.88 ± 0.18
Lignosulfonate	598 ± 73	12.06 ± 0.69	3.22 ± 0.16
Organosolv lignin	604 ± 58	11.75 ± 1.19	16.86 ± 2.68
Polycaprolactone without filler	354 ± 20	28.16 ± 3.64	696.61 ± 74.75



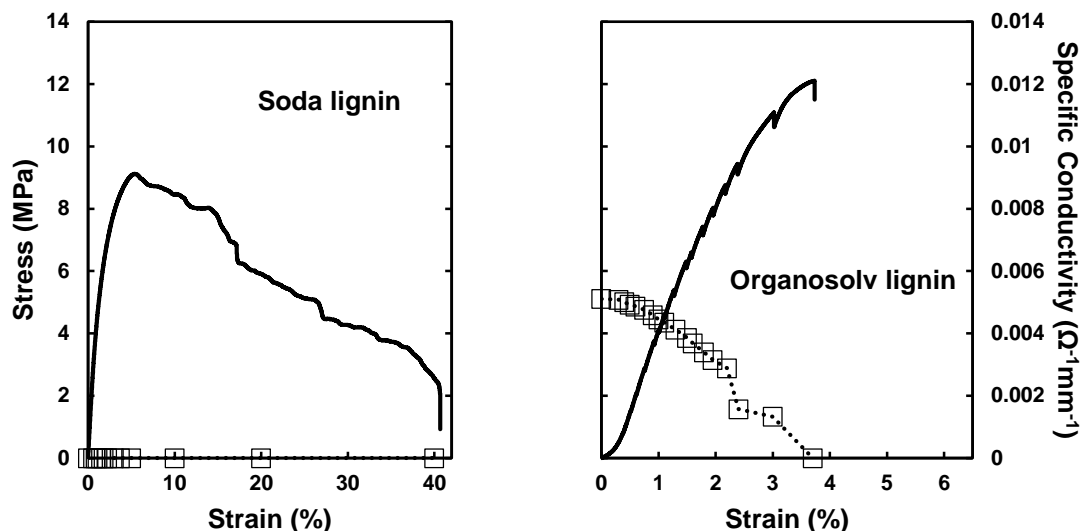


Fig. 11. Stress and specific conductivity of the PCL-carbon composite during the step-wise tensile testing: (a) kraft lignin; (b) liginosulfonate; (c) soda lignin; and (d) organosolv lignin

The PCL-carbon composite films filled with 30% carbon showed remarkably different electrical conductivity values (Fig. 11). First, the poor conductivity of the liginosulfonate-based variant correlated well with the poor conductivity of the liginosulfonate-derived carbon powder (Fig. 10). Considering the conductivity values measured for the carbon powders, the absence of conductivity in the films filled with the soda lignin-derived carbon was surprising. However, it had to be considered that to achieve a strong conductivity, a particulate filler must be both conductive and able to dispose of a high specific volume to enable the formation of a percolating filler network within a polymeric matrix. Because soda lignin-derived carbon was of a considerably higher density compared with all of the other variants (Fig. 9), it was concluded that the soda lignin-derived carbon lacked the volume filling required to achieve percolation at the given mass-based filling ratio. For the remaining variants derived from kraft and organosolv lignin, appreciable electric conductivity values were achieved. Upon stretching the carbon-filled polymer films, the conductivity decreased because the stiffer carbon particles experienced less strain than the surrounding polymer matrix, which resulted in less particle-to-particle contact and reduced the conductivity with an increasing tensile strain on the composite (Celzard *et al.* 2002; Chung 2004).

CONCLUSIONS

1. The characterisations of the properties and structures of the carbons produced by carbonisation of four different lignin samples indicated that the properties and structure depended on the lignin type and carbonisation temperature.
2. In all of the carbon powders, the graphitic structures were highly disordered. The liginosulfonate-derived carbon in particular showed a poor performance in terms of the electrical conductivity.

3. The kraft lignin- and organosolv lignin-derived carbons were shown to be suitable in principle for application as functional fillers in polymers, even exhibiting strain sensing capability.

ACKNOWLEDGMENTS

The authors are grateful for the funding from the Austrian Science Promotion Agency (FFG) (Bridge Project 846543). Part of this work was carried out within the project BioCarb-K, co-financed by the European Regional Development Fund (EFRE) and the province of Upper Austria through the programme IWB 2014-2020.

REFERENCES CITED

- Ago, M., Borghei, M., Haataja, J. S., and Rojas, O. J. (2016). "Mesoporous carbon soft-templated from lignin nanofiber networks: Microphase separation boosts supercapacitance in conductive electrodes," *RSC Adv.* 6(89), 85802-85810. DOI: 10.1039/C6RA17536H
- Areskog, D., Li, J., Gellerstedt, G., and Henriksson, G. (2010). "Investigation of the molecular weight increase of commercial lignosulfonates by laccase catalysis," *Biomacromolecules* 11(4), 904-910. DOI: 10.1021/bm901258v
- Balberg, I. (2002). "A comprehensive picture of the electrical phenomena in carbon black-polymer composites," *Carbon* 40(2), 139-143. DOI: 10.1016/S0008-6223(01)00164-6
- Betancur, M., Bonelli, P. R., Velásquez, J. A., and Cukierman, A. L. (2009). "Potentiality of lignin from the kraft pulping process for removal of trace nickel from wastewater: Effect of demineralisation," *Bioresour. Technol.* 100(3), 1130-1137. DOI: 10.1016/j.biortech.2008.08.023
- Boerjan, W., Ralph, J., and Baucher, M. (2003). "Lignin biosynthesis," *Annu. Rev. Plant Biol.* 54, 519-546. DOI: 10.1146/annurev.arplant.54.031902.134938
- Bourrat, X. (1993). "Electrically conductive grades of carbon black: Structure and properties," *Carbon* 31(2), 287-302. DOI: 10.1016/0008-6223(93)90034-8
- Braun, J. L., Holtman, K. M., and Kadla, J. F. (2005). "Lignin-based carbon fibers: Oxidative thermostabilization of kraft lignin," *Carbon* 43(2), 385-394. DOI: 10.1016/j.carbon.2004.09.027
- Bruijninx, P. C. A., Rinaldi, R., and Weckhuysen, B. M. (2015). "Unlocking the potential of a sleeping giant: Lignins as sustainable raw materials for renewable fuels, chemicals and materials," *Green Chem.* 17(11), 4860-4861. DOI: 10.1039/C5GC90055G
- Castellino, M., Rovere, M., Shahzad, M. I., and Tagliaferro, A. (2016) "Conductivity in carbon nanotube polymer composites: A comparison between model and experiment." *Compos. Part A* 87, 237-242. DOI: 10.1016/j.compositesa.2016.05.002
- Celzard, A., Marêché, J. F., Payot, F., and Furdin, G. (2002). "Electrical conductivity of carbonaceous powders," *Carbon* 40(15), 2801-2815. DOI: 10.1016/S0008-6223(02)00196-3

- Çetin, N. S., and Özmen, N. (2002). "Use of organosolv lignin in phenol–formaldehyde resins for particleboard production: I. Organosolv lignin modified resins," *Int. J. Adhes. Adhes.* 22(6), 477-480. DOI: 10.1016/S0143-7496(02)00058-1
- Chakar, F. S., and Ragauskas, A. J. (2004). "Review of current and future softwood kraft lignin process chemistry," *Ind. Crop. Prod.* 20(2), 131-141. DOI: 10.1016/j.indcrop.2004.04.016
- Chatterjee, S., Saito, T., Rios, O., and Johs, A. (2014). "Lignin based carbon materials for energy storage applications," in: *Green Technologies for the Environment*, American Chemical Society, Washington, DC, pp. 203-218.
- Chung, D. D. L. (2004). "Electrical applications of carbon materials," *J. Mater. Sci.* 39(8), 2645-2661. DOI: 10.1023/B:JMASC.0000021439.18202.ea
- Das, T. K., and Prusty, S. (2012). "Review on conducting polymers and their applications." *Polym. Plastics Technol. Eng.* 51, 1487-1500. DOI: 10.1080/03602559.2012.710697
- Doherty, W. O. S., Mousavioun, P., and Fellows, C. M. (2011). "Value-adding to cellulosic ethanol: Lignin polymers," *Ind. Crop. Prod.* 33(2), 259-276. DOI: 10.1016/j.indcrop.2010.10.022
- Dresselhaus, M. S., Jorio, A., Hofmann, M., Dresselhaus, G., and Saito, R. (2010). "Perspectives on carbon nanotubes and graphene Raman spectroscopy," *Nano Lett.* 10(3), 751-758. DOI: 10.1021/nl904286r
- Duval, A., and Lawoko, M. (2014). "A review on lignin-based polymeric, micro- and nano-structured materials," *React. Funct. Polym.* 85, 78-96. DOI: 10.1016/j.reactfunctpolym.2014.09.017
- Foston, M., Nunnery, G. A., Meng, X., Sun, Q., Baker, F. S., and Ragauskas, A. (2013). "NMR a critical tool to study the production of carbon fiber from lignin," *Carbon* 52, 65-73. DOI: 10.1016/j.carbon.2012.09.006
- Fu, S.-Y., Feng, X.-Q., Lauke, B., and Mai, Y.-W. (2008). "Effects of particle size, particle/matrix interface adhesion and particle loading on mechanical properties of particulate–polymer composites," *Compos. Part B-Eng.* 39(6), 933-961. DOI: 10.1016/j.compositesb.2008.01.002
- García, A., Toledano, A., Serrano, L., Egüés, I., González, M., Marín, F., and Labidi, J. (2009). "Characterization of lignins obtained by selective precipitation," *Sep. Purif. Technol.* 68(2), 193-198. DOI: 10.1016/j.seppur.2009.05.001
- Gindl-Altmutter, W., Fürst, C., Mahendran, A., Obersriebnig, M., Emsenhuber, G., Kluge, M., Veigel, S., Keckes, J., and Liebner, F. (2015). "Electrically conductive kraft lignin-based carbon filler for polymers," *Carbon* 89, 161-168. DOI: 10.1016/j.carbon.2015.03.042
- Gonugunta, P., Vivekanandhan, S., Mohanty, A. K., and Misra, M. (2012). "A study on synthesis and characterization of biobased carbon nanoparticles from lignin," *World Journal of Nano Science and Engineering* 2(3), 148-153. DOI: 10.4236/wjnse.2012.23019
- González-García, S., Moreira, M. T., Artal, G., Maldonado, L., and Feijoo, G. (2010). "Environmental impact assessment of non-wood based pulp production by soda-anthraquinone pulping process," *J. Clean. Prod.* 18(2), 137-145. DOI: 10.1016/j.jclepro.2009.10.008
- Gosselink, R. J. A., de Jong, E., Guran, B., and Abächerli, A. (2004). "Co-ordination network for lignin—Standardisation, production and applications adapted to market requirements (EUROLIGNIN)," *Ind. Crop. Prod.* 20(2), 121-129. DOI: 10.1016/j.indcrop.2004.04.015

- Hayashi, J., Kazehaya, A., Muroyama, K., and Watkinson, A. P. (2000). "Preparation of activated carbon from lignin by chemical activation," *Carbon* 38(13), 1873-1878. DOI: 10.1016/S0008-6223(00)00027-0
- Huang, J.-C. (2002). "Carbon black filled conducting polymers and polymer blends," *Adv. Polym. Tech.* 21(4), 299-313. DOI: 10.1002/adv.10025
- Jin, J., Lin, Y., Song, M., Gui, C., and S. Leesirisan (2013). "Enhancing the electrical conductivity of polymer composites," *Eur. Polym. J.* 49(5), 1066-1072. DOI: 10.1016/j.eurpolymj.2013.01.014
- Kadla, J. F., Kubo, S., Venditti, R. A., Gilbert, R. D., Compere, A. L., and Griffith, W. (2002). "Lignin-based carbon fibers for composite fiber applications," *Carbon* 40(15), 2913-2920. DOI: 10.1016/S0008-6223(02)00248-8
- Kai, D., Tan, M. J., Chee, P. L., Chua, Y. K., Yap, Y. L., and Loh, X. J. (2016). "Towards lignin-based functional materials in a sustainable world," *Green Chem.* 18(5), 1175-1200. DOI: 10.1039/C5GC02616D
- Köhnke, J., Fürst, C., Unterweger, C., Rennhofer, H., Lichtenegger, H. C., Keckes, J., Emsenhuber, G., Mahendran, A., Liebner, F., and Gindl-Altmutter, W. (2016). "Carbon microparticles from organosolv lignin as filler for conducting poly(lactic acid)," *Polymers* 8(6), 205-217. DOI: 10.3390/polym8060205
- Köhnke, J., Rennhofer, H., Lichtenegger, H., Mahendran, A., Unterweger, C., Prats-Mateu, B., Gierlinger, N., Schwaiger, E., Mahler, A.-K., Potthast, A., *et al.* (2018). "Electrically conducting carbon microparticles by direct carbonization of spent wood pulping liquor," *ACS Sustain. Chem. Eng.* 6(3), 3385-3391. DOI: 10.1021/acssuschemeng.7b03582
- Laurichesse, S., and Avérous, L. (2014). "Chemical modification of lignins: Towards biobased polymers," *Prog. Polym. Sci.* 39(7), 1266-1290. DOI: 10.1016/j.progpolymsci.2013.11.004
- Li, F., Qi, L., Yang, J., Xu, M., Luo, X., and Ma, D. (2000). "Polyurethane/conducting carbon black composites: Structure, electric conductivity, strain recovery behavior, and their relationships," *J. Appl. Polym. Sci.* 75(1), 68-77. DOI: 10.1002/(SICI)1097-4628(20000103)75:1<68::AID-APP8>3.0.CO;2-I
- Liu, W.-J., Jiang, H., and Yu, H.-Q. (2015). "Thermochemical conversion of lignin to functional materials: A review and future directions," *Green Chem.* 17(11), 4888-4907. DOI: 10.1039/C5GC01054C
- Mansouri, N.-E. E., and Salvadó, J. (2006). "Structural characterization of technical lignins for the production of adhesives: Application to lignosulfonate, kraft, soda-anthraquinone, organosolv and ethanol process lignins," *Ind. Crop. Prod.* 24(1), 8-16. DOI: 10.1016/j.indcrop.2005.10.002
- Norberg, I., Nordström, Y., Drougge, R., Gellerstedt, G., and Sjöholm, E. (2013). "A new method for stabilizing softwood kraft lignin fibers for carbon fiber production," *J. Appl. Polym. Sci.* 128(6), 3824-3830. DOI: 10.1002/app.38588
- Pan, X., Arato, C., Gilkes, N., Gregg, D., Mabee, W., Pye, K., Xiao, Z., Zhang, X., and Saddler, J. (2005). "Biorefining of softwoods using ethanol organosolv pulping: Preliminary evaluation of process streams for manufacture of fuel-grade ethanol and co-products," *Biotechnol. Bioeng.* 90(4), 473-481. DOI: 10.1002/bit.20453
- Rodríguez, A., Sánchez, R., Requejo, A., and Ferrer, A. (2010). "Feasibility of rice straw as a raw material for the production of soda cellulose pulp," *J. Clean. Prod.* 18(10-11), 1084-1091. DOI: 10.1016/j.jclepro.2010.03.011

- Ruiz-Rosas, R., Bedia, J., Lallave, M., Loscertales, I. G., Barrero, A., Rodríguez-Mirasol, J., and Cordero, T. (2010). "The production of submicron diameter carbon fibers by the electrospinning of lignin," *Carbon* 48(3), 696-705. DOI: 10.1016/j.carbon.2009.10.014
- Sadezky, A., Muckenhuber, H., Grothe, H., Niessner, R., and Pöschl, U. (2005). "Raman microspectroscopy of soot and related carbonaceous materials: Spectral analysis and structural information," *Carbon* 43(8), 1731-1742. DOI: 10.1016/j.carbon.2005.02.018
- Sánchez-González, J., Macías-García, A., Alexandre-Franco, M. F., and Gómez-Serrano, V. (2005). "Electrical conductivity of carbon blacks under compression," *Carbon* 43(4), 741-747. DOI: 10.1016/j.carbon.2004.10.045
- Shulga, G., Rekner, F., and Varslavan, J. (2001). "SW—Soil and water: Lignin-based interpolymer complexes as a novel adhesive for protection against erosion of sandy soil," *J. Agr. Eng. Res.* 78(3), 309-316. DOI: 10.1006/jaer.2000.0599
- Sixta, H. (2006). *Handbook of Pulp*, Wiley-VCH Verlag GmbH, Weinheim, Germany.
- Snowdon, M. R., Mohanty, A. K., and Misra, M. (2014). "A study of carbonized lignin as an alternative to carbon black," *ACS Sustain. Chem. Eng.* 2(5), 1257-1263. DOI: 10.1021/sc500086v
- Song, K., Ganguly, I., Eastin, I., and Dichiara, A. B. (2017). "Lignin-modified carbon nanotube/graphene hybrid coating as efficient flame retardant," *Int. J. Mol. Sci.* 18(11), 2368-2381. DOI: 10.3390/ijms18112368
- Suhas, Carrott, P. J. M., and Carrott, M. M. L. R. (2007). "Lignin—From natural adsorbent to activated carbon: A review," *Bioresource Technol.* 98(12), 2301-2312. DOI: 10.1016/j.biortech.2006.08.008
- Tejado, A., Peña, C., Labidi, J., Echeverria, J. M., and Mondragon, I. (2007). "Physico-chemical characterization of lignins from different sources for use in phenol-formaldehyde resin synthesis," *Bioresource Technol.* 98(8), 1655-1663. DOI: 10.1016/j.biortech.2006.05.042
- Thakur, V. K., Thakur, M. K., Raghavan, P., and Kessler, M. R. (2014). "Progress in green polymer composites from lignin for multifunctional applications: A review," *ACS Sustain. Chem. Eng.* 2(5), 1072-1092. DOI: 10.1021/sc500087z
- Tuinstra, F., and Koenig, J. L. (1970). "Raman spectrum of graphite," *J. Chem. Phys.* 53(3), 1126-1130. DOI: 10.1063/1.1674108
- Vainio, U., Maximova, N., Hortling, B., Laine, J., Stenius, P., Simola, L. K., Gravitis, J., and Serimaa, R. (2004). "Morphology of dry lignins and size and shape of dissolved kraft lignin particles by X-ray scattering," *Langmuir* 20(22), 9736-9744. DOI: 10.1021/la048407v
- Wang, M., Leitch, M., and Xu, C. (2009). "Synthesis of phenol-formaldehyde resol resins using organosolv pine lignins," *Eur. Polym. J.* 45(12), 3380-3388. DOI: 10.1016/j.eurpolymj.2009.10.003
- Woodruff, M. A., and Hutmacher, D. W. (2010). "The return of a forgotten polymer—Polycaprolactone in the 21st century," *Prog. Polym. Sci.* 35(10), 1217-1256. DOI: 10.1016/j.progpolymsci.2010.04.002
- Xu, C., Arancon, R. A. D., Labidi, J., and Luque, R. (2014). "Lignin depolymerisation strategies: Towards valuable chemicals and fuels," *Chem. Soc. Rev.* 43(22), 7485-7500. DOI: 10.1039/C4CS00235K

- Yang, D., Qiu, X., Zhou, M., and Lou, H. (2007). "Properties of sodium lignosulfonate as dispersant of coal water slurry," *Energ. Convers. Manage.* 48(9), 2433-2438. DOI: 10.1016/j.enconman.2007.04.007
- Yi, X., He, W., Zhang, X., Yue, Y., Yang, G., Wang, Z., Zhou, M., and Wang, L. (2017). "Graphene-like carbon sheet/Fe₃O₄ nanocomposites derived from soda papermaking black liquor for high performance lithium ion batteries," *Electrochim. Acta* 232, 550-560. DOI: 10.1016/j.electacta.2017.02.130

Article submitted: June 7, 2018; Peer review completed: July 30, 2018; Revisions accepted: December 12, 2018; Published: December 13, 2018.
DOI: 10.15376/biores.14.1.1091-1109